

Light Bullet Mode-Locking In Waveguide Arrays

Matt Williams and J. Nathan Kutz,

Abstract—A theoretical proposal is presented for the generation of mode-locked light-bullets in planar waveguide arrays, extending the concept of time-domain mode-locking in waveguide arrays to spatial (transverse) mode-locking in slab waveguides. The model presented yields three-dimensional localized states that act as global attractors to the waveguide array system. Single pulse stationary and time-periodic solutions as well as the transition to multi-pulse solutions as a function of gain are observed to be stabilized in such a system.

I. INTRODUCTION

Semiconductor waveguide arrays (WGAs) are of significant technological interest in the broader photonics community due to their inherently nonlinear response to an intense applied electric field [1], [2]. Indeed, the spatial self-focusing and nonlinear mode-coupling (NLMC) exhibited by the WGAs have led to their consideration as ideal photonic devices for all-optical signal processing (routine and switching) in fiber optic networks and devices [3], [4], [5], [6], pulse reshaping [7], [8], continuous-wave lasing [9], as well as a discrete form of Kerr lensing (nonlinear saturable absorption) in a mode-locked laser cavity [10], [11]. In the latter application, theoretical studies show the WGA can be used with great success to create passively mode-locked fiber laser cavities capable of generating high-power, ultra-short pulses in both the normal and anomalous dispersion regimes [12], [13]. In such mode-locking, the stable pulses are generated by a fundamental balance of chromatic dispersion and self-phase modulation [10], [11], [12], [13]. The extension of this mode-locking concept to constructing a modelocked laser on a chip architecture are readily apparent. Indeed, significant effort has gone into the modeling and characterization of such arrays and their nonlinear mode-coupling (NLMC) properties [7], [13]. These methods predict and characterize the NLMC driven mode-locking in the quasi one-dimensional geometry of a ridge waveguide array. The extension of the one-dimensional geometry to two spatial dimensions follows naturally when the confinement occurs in a planar geometry, and the creation of transverse-dimensional light bullets, or cavity solitons, is desirable. Note that in this analysis the vertical confinement in the waveguide is averaged over and not dealt with explicitly. However, the vertical confinement in conjunction with transverse confinement creates the desired three-dimensional localized coherent structure or light bullet. In this paper, we theoretically analyze an approach to producing spatial mode-locked light bullets in a physically based but heuristically motivated model of a planar waveguide structure. The planar geometry confinement and two transverse dimensions mode-lock pulses by a fundamental balance of spatial diffraction

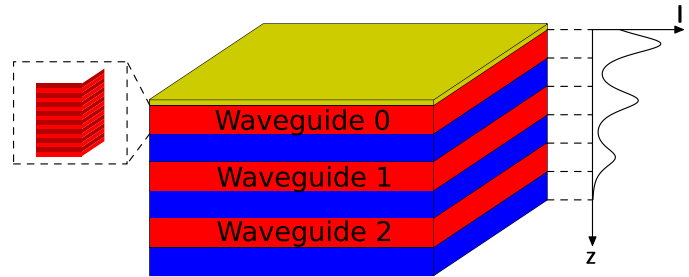


Fig. 1. A schematic of the two-dimensional waveguide array. The waveguides, shown in red, are separated by low-index insulating regions. The proposed structure of the waveguides are a Bragg grating structure, shown to the left. Gain is applied to waveguide 0 by means of an injection current created by biasing the conducting contact (See Ref. [9] for recent experiments). Additionally, attenuation is applied only to waveguide 2. The prototypical vertical distribution of the intensity is shown on the right. The Bragg grating structure confines the fields to the waveguides with weak evanescent coupling allowing energy transfer.

and self-phase modulation. The light-bullets considered here are self-organizing (from white-noise initial conditions) and stabilized in the transverse dimension via the NLMC in the planar waveguide geometry. Further, the light-bullets generated are in a cavity-less configuration since no mirrors are used to form a cavity or ring geometry. The mode-locking is robust under perturbation and self-starting, suggesting it may be an ideal photonic device for numerous all-optical applications. This adds yet another potential method and technology for generating localized cavity-like solitons [14].

All the technological aspects currently exist to generate the aforementioned mode-locked light bullets. Figure 1 illustrates a prototypical example of a waveguide geometry that may be suitable and appropriate for such purposes. Instead of the typical ridge waveguide array structure [1], a vertical cavity surface emitting laser (VCSEL) type slab geometry is envisioned. In some respects, this overlaps the theoretical concepts used in the experimentally realized broad-area VCSEL configuration which has been demonstrated to produce cavity solitons [15]. However, no cavity [15] or broad-area holding beam is required [16], [17], [18], [19] in the technology advocated here. Thus unlike the standard VCSEL, which is often used as a mirror and quantum saturable absorber for standard mode-locking of ultra-short (in time) pulses (See, for instance, [20] and references therein), the WGA slab structure does not confine the field to single-mode operation in the transverse direction. Instead, the transverse field is allowed to be large (in comparison to the single-mode diameter) and unconfined. In the third dimension, the propagation direction, the Bragg grating type structure is assumed to be sufficient to create a stationary Bragg soliton in each of the three planar waveguides so that the field is confined in waveguides zero, one, and two respectively (See Fig. 1). The zero group-velocity

M. Williams and J. N. Kutz are with the Department of Applied Mathematics, University of Washington, Seattle, WA 98195-2420

soliton, which has been considered in the context of slow light, has been obtained theoretically and is a goal of ongoing experimental work [21], [22]. In recent years, the use of defects in a fiber Bragg Grating has been studied as a mechanism for trapping Bragg solitons [23]. The use of such defects in slab waveguide arrays provides an alternate way to generate an effectively zero group-velocity pulse. The coupling of energy between adjacent waveguide slabs is described by the standard mode-coupling theory of evanescent field interactions [24]. While certainly different physical situations, the extension of the waveguide array mode-locking model (WGAML) is robust enough to capture both arrangements using the same governing equations [11], [12]. Using the simplified version of the extended WGAML, the dynamics of the slab waveguide array are studied for both negative and positive refractive index slabs. It will be shown that in a particular parameter region, light-bullets evolve naturally from white-noise. Additionally, the transition from single pulse, to breathing, and finally to multiple light-bullets will be explored via a simple increase in the gain applied to the system.

The paper is outlined as follows: In Sec. 2 the governing equations are given along with their relevant parameters. The mode-locking dynamics are explored in Sec. 3, initially with the development of radially symmetry mode-locked solutions, and then with the full dynamics along with its transition from one-to-two light bullets, i.e. the multi-pulsing transition which occurs as a function of increased cavity gain. A brief summary of the results and its technological outlook is outlined in Sec. 4.

II. GOVERNING EQUATIONS

Mode-locking in waveguide arrays is driven by the competition between the saturable absorption behavior generated by NLMC [13] of the waveguides along with an applied bandwidth limited gain. The WGAML, which describes temporal mode-locking in ridge waveguide arrays, has been heuristically extended from one to two spatial dimensions by replacing the one-dimensional derivative and norm operators with their two-dimensional analogs. However, as eluded to in the introduction, the heuristic extension models systems that are quite physical. One such system is the spatially extended VCSEL-type architecture system in Fig. 1. The governing equations for this physical configuration are:

$$i\frac{\partial A_0}{\partial t} + \frac{D}{2}\nabla^2 A_0 + \beta|A_0|^2 A_0 + C A_1 + i\gamma_0 A_0 - ig(t)(1 + \tau\nabla^2) A_0 + i\rho|A_0|^4 A_0 = 0 \quad (1a)$$

$$i\frac{\partial A_1}{\partial t} + C(A_0 + A_2) + i\gamma_1 A_1 = 0 \quad (1b)$$

$$i\frac{\partial A_2}{\partial t} + C A_1 + i\gamma_2 A_2 = 0 \quad (1c)$$

where $\nabla^2 = \partial_x^2 + \partial_y^2$ and

$$g(t) = \frac{2g_0}{1 + ||A_0||^2/e_0}. \quad (2)$$

Here A_0 , A_1 , and A_2 are the envelope of the electric fields in the 0th, 1st and 2nd waveguides respectively. The parameter D is the diffraction coefficient in each of the slab arrays.

Assuming the material is isotropic, the proper choice of non-dimensional variables gives $D = -1$ or 1 for negative or positive index of refraction respectively. The parameter β is the strength of self-phase modulation, ρ is proportional to the probability of three-photon absorption, γ_j is the coefficient of linear attenuation in each waveguide, and C is proportional to the strength of the coupling between waveguides and is the average value of the overlap integral as calculated in standard coupled mode theory [24]. Details of the scalings can be found in Ref. [13]. The saturable gain coefficient $g(t)$, shown in (2), accounts for the depletion of minority charge carriers at high optical intensities. The $g(t)\nabla^2$ term prohibits the growth of high frequency spatial modes via the bandwidth limiting parameter τ . The damping of high frequency spatial modes is implied by the presence of diffusion in the charge carrier equations often found in full charge carrier models [25].

This physical interpretation of the WGAML differs from that of Proctor and Kutz [11] in two ways: First, D represents diffraction instead of chromatic dispersion. The mode-locked light-bullets are transversely generated and stabilized versus localized time pulses in standard mode-locking. While D is positive for positive index materials, it has been shown by Kockaert and coworkers [26] that negative index materials have a nonlinear Schrödinger-based model with a negative D . Therefore, a negative value of D is taken to mean the index of refraction is negative in the guiding regions. A second difference is the nature of the coupled modes. Typically, the coupled modes of a waveguide array are the guided modes of each individual waveguide [24]. In a VCSEL configuration, the coupled modes are the stationary or trapped Bragg solitons in each of the waveguides. Coupled mode theory is applicable provided the coupling between slab waveguides remains weak. Therefore, the distinction between truly zero group-velocity modes, trapped modes, or stationary modes produced by another approach is isolated to changes in the value of C [22], [23]. While the extension from one time dimension to two transverse spatial dimensions was motivated by heuristics, the resulting model has a clear physical interpretation. In particular, the variables A_0 , A_1 , and A_2 represent the spatial, transverse amplitude of trapped Bragg solitons in each of waveguides, and the sign of the dispersion reflects the sign of the index of refraction of the guiding region.

III. MODE-LOCKED DYNAMICS

The dynamical behavior of this system is critically dependent upon the gain parameter g_0 that acts as the bifurcation parameter that governs the transition from stable single-pulses, to time-periodic breathing solutions, and finally to multiple pulse solutions [12]. Due to the isotropy of the system, it is assumed that a steady state output pulse will also possess radial symmetry. Indeed, for single- and multiple-pulse stationary solutions this simplification agrees quite well with simulations of the fully two-dimensional problem. However, this simplification performs poorly in time-periodic and other non-static cases due to the generation of a non-radial noise background that breaks the radial symmetry. Regardless, the radially symmetric solutions provide an excellent starting point for considering light-bullet solutions.

A. Radially Symmetric Solutions

The radially symmetric solutions are an important class of stationary solutions to the modified WGAML equation because radially symmetry allows the reduction of the governing partial differential equation system (1) from two spatial-dimensions to one spatial dimension in the radial variable. This simplifies the analysis and makes the study of the dynamics more numerically tractable. In the radially symmetric case, the system was discretized in space using a second order finite-difference scheme for the spatial derivatives with 512 points on a domain of size 30. Additionally, Neumann and Dirichlet conditions were used for the $r = 0$ and $r = 30$ conditions respectively. The system is evolved in time using the standard 4th order Runge-Kutta methods in MATLAB. This allows a relatively quick method for exploring the parameter space.

With the proper parameters, negative index waveguides (defocusing, or normal, nonlinear Schrödinger) are capable of producing stable pulses from noise. Figure 2 demonstrates the radially-symmetric mode-locked solution supported in a three-slab waveguide array structure starting from initial white noise in the 0th waveguide and no energy in waveguides 1 and 2. This particular initial condition was chosen to mimic experimental conditions. However, as white-noise possesses all spatial wavenumbers, this initial condition is guaranteed to possess the specific modes that are amplified by the modulational instabilities of the zero solution. The modulational instability generates long-wavelength structures in the spatial domain which then develop into a single localized structure due to the restriction of the cavity energy restrictions of the saturable gain. Shown in Fig. 2 are the generated electric field envelopes in all three waveguides for the parameter values

$$(D, C, \gamma_0, \gamma_1, \gamma_2, e_0, \tau, p, g_0) = (-1, 10, 0, 0, 10, 1, 0.1, 1, 35). \quad (3)$$

These coefficients corresponds to a negative index waveguiding regions with attenuation applied in waveguide 2 and bandwidth-limited amplification applied in waveguide 0. As gain is only applied in the 0th waveguide, the mode-shapes of the 1st and 2nd waveguides are inherited from the 0th waveguide. This is consistent with findings in the one-dimensional case [12]. This single-pulse solution is robust and persists for a relatively wide range of gains. As the pulse forms from noise, it is stable with respect to large perturbations of the steady state solution. It appears that the single-pulse mode-locked state is a global attractor of the system for the specific value of gain g_0 chosen.

The positive index case (focusing or anomalous nonlinear Schrödinger) requires a more careful selection of parameter values due to the self-focusing and collapse that is inherent in the two-dimensional nonlinear Schrödinger operator of Eq. (1a). Indeed, it is critical in this case to include the physically relevant effects of three-photon absorption in order to avoid the mathematical collapse and blow-up of the solution. The following parameters were used for the positive index case:

$$(D, C, \gamma_0, \gamma_1, \gamma_2, e_0, \tau, p, g_0) = (1, 5, 1, 1, 10, 1, 0.08, 0.5, 4.88). \quad (4)$$

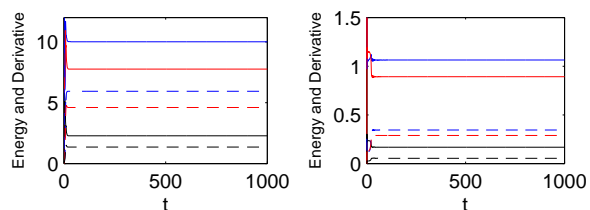


Fig. 4. The energy and derivative fluctuations for the negative diffraction (left) and positive diffraction (right) regimes. After an initial transient of tens of time units, the norms settle to a steady state indicating a stationary pulse. The solid lines are the energy and the dotted lines are the derivative fluctuations. The blue lines correspond to waveguide 0 data, the red lines to waveguide 1 data, and the black lines correspond to waveguide 2 data.

The switch from negative to positive index materials has a large impact upon the resulting dynamics and parameters required to obtain mode-locking. However, mode-locked solutions can be achieved as Fig. 3 shows. Additionally, the solutions are stable with respect to perturbations of the steady state solution. In these numerical simulations, the initial condition used is a hyperbolic secant as opposed to white-noise. This was done to circumvent numerical difficulties that arise due to the approximation of a Cauchy problem on a finite domain. At low amplitudes, the leading order solutions are Bessel functions. However, Bessel functions represent infinite energy solutions to the Cauchy problem, and are thus spurious solutions produced by the numerics. While no numerical solutions have been obtained that form from noise, this in no way implies that positive index materials are unable to be used for passive mode-locking. This is simply a mathematical difficulty in the reduction of the problem to radial coordinates.

Regardless of the initial condition, the pulses that form are true mode-locked light bullets. To help illustrate the mode-locking formation, Fig. 4 plots the energy ($\|A_j\|^2 = \int_{-\infty}^{\infty} \int_{-\infty}^{\infty} |A_j|^2 dx dy$) and derivative ($\|\nabla A_j\|^2$) fluctuations for both the positive and negative index cases. The energy and solution derivative, or mathematically the L_2 and H_1 norms, are shown to quickly settle to a steady state. Hence, the radial solutions evolve to a steady state which is the mode-locked light bullet.

The radially symmetric solutions give a great deal of insight into the underlying stable structures in the system. However, what is most important is the full dynamics of Eq. (1) without the assumption of radial symmetry. Specifically, whether or not the radially symmetric solutions spontaneously arise from non-radially symmetric initial conditions. Relaxing the radial symmetry assumption and repeating the computation with both spatial dimensions and a white-noise initial condition, the system again evolves to a steady state as shown in Fig. 5 for the parameters considered in Fig. 2. For this result, a pseudo-spectral method was used in space with the same Runge-Kutta method to evolve the system in time. Spatially, 256 points were used in each of the spatial directions on a square domain of length 80. The quantitative similarities in the mode-locked solution in comparison to the radially symmetric solution show that the radial approximation is an accurate and valid representation of the true solution in the stable case.

The dynamical evolution and mode-locking formation dy-

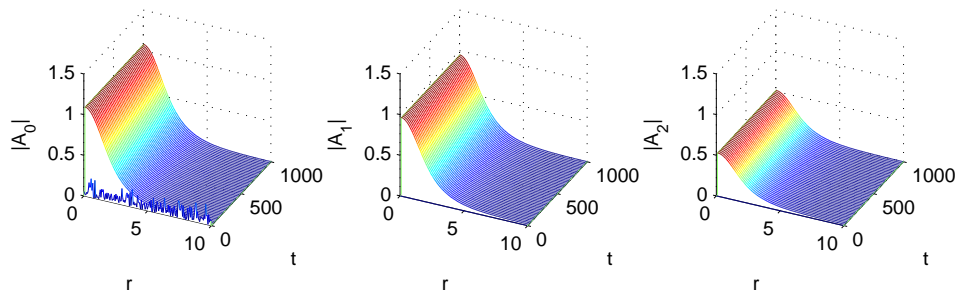


Fig. 2. Radial optical field amplitudes for the negative diffraction regime in the 0th, 1st, and 2nd waveguides respectively. Consistent with the assumptions of the model, the fields in waveguides 1 and 2 have inherited their shape from waveguide 0. Note that the radial solution forms from a white-noise initial condition in waveguide 0.

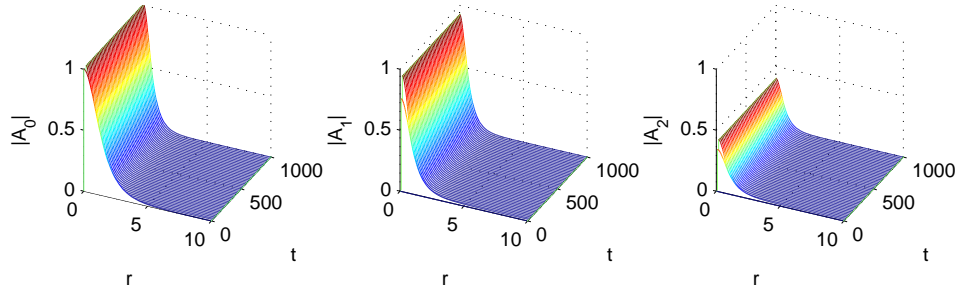


Fig. 3. Optical field amplitudes in the positive diffraction regime in the 0th, 1st, and 2nd waveguides respectively. Compared to the results in Fig. 2, this pulse is obtained for far lower values of gain. In this case, this initial condition is a hyperbolic secant pulse in each of the waveguides.

namics for the full system of equations (1) with (2) is illustrated in the first movie (Media 1). The parameters used are identical to those of Fig. 5. The four panel movie illustrates the intensity dynamics in waveguide 0 (top left) as well as waveguides 1 and 2 (bottom left). Note that that the field in the first waveguide has been uniformly raised by 1.5 for illustrative purposes. The energy in the waveguides and the spectrum of the 0th waveguide solution are shown in the top and bottom right panels respectively.

B. Time Periodic Solutions: Breathers

For larger values of gain g_0 , the system undergoes what is conjectured to be a Hopf Bifurcation and transitions from stationary solutions to time-periodic breather solutions. This conjecture is based upon recent stability analysis findings in one-dimension [12] for which the Hopf bifurcation can be concluded explicitly. In two dimensions, these solutions are characterized by an oscillating radial pulse and a noise background. The noise background cannot be represented radially, creating a discrepancy between the radial and fully two-dimensional analysis. Due to this difference, two sets of parameters were used. For the radial analysis, the coefficients used were:

$$(D, C, \gamma_0, \gamma_1, \gamma_2, e_0, \tau, p, g_0) = (-1, 10, 0, 0, 10, 1, 0.1, 1, 50), \quad (5)$$

but in the full two-dimensional governing model Eq. (1), $g_0 = 60$ in order to account for energy supplied to the noise background not present in the radially symmetric reduction. Solving the radial problem numerically produces the breather solution shown in Fig. 6. This solution is periodic and forms from noise. The oscillation can be noticed most clearly via

the energy fluctuations in the middle panel of the figure. The oscillations take place on two distinct timescales. The slow oscillations are visible on the amplitude plot and the plot of energy fluctuations. The fast timescale may be seen there too, but exhibits itself in the lack of smoothness on the amplitude plot and the thickness of the lines in the energy fluctuation plots.

The dynamics of the full, non-radially symmetric system for the two-dimensional case are similar in character, but different in quantitative values. Even with the larger gain of the system, the energy fluctuations for the two-dimensional case shown in Fig. 6 in the right panel exhibit smaller amplitude oscillations than in the radial case. However, they do possess the same fast and slow timescales of oscillation seen in the radial case. The difference is again due to the non-radial noise background. This appears to consume the energy that normally would force the pulse to oscillate. We are currently investigating the role of the CW noise background and its facilitation and/or suppression of mode-locking of light bullets.

C. Multi-Pulsing Transition

Increasing the gain to even higher values of g_0 , the breathing one-pulse solution becomes unstable. At that point, multiple-pulse solutions obtain stability and become the dominant solution type. The explanation for this behavior is similar to that observed by Kutz and Standstede [12], who studied the loss of stability of the breather solutions and also the stability of non-interacting multiple-pulse solutions. An example of the splitting process for this particular array is shown in Fig. 7. In the first three frames, the single pulse splits into two, but the interaction between the newly formed pair of pulses causes them to recombine into a single pulse. For sufficiently long

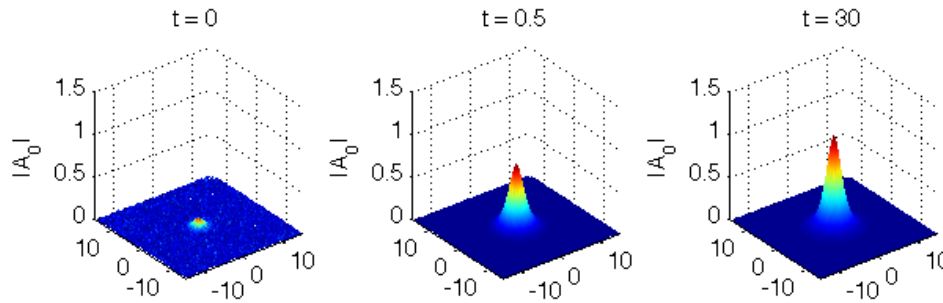


Fig. 5. Formation of a radially symmetric mode-locked solution in the negative diffraction regime starting from seeded white-noise. The intermediate image shows the presence of both noise and a hyperbolic-secant like pulse. The intensity discrimination and saturating gain eliminate the background noise. This full simulation is the proto-typical mode-locking behavior expected in the slab waveguide array structure.

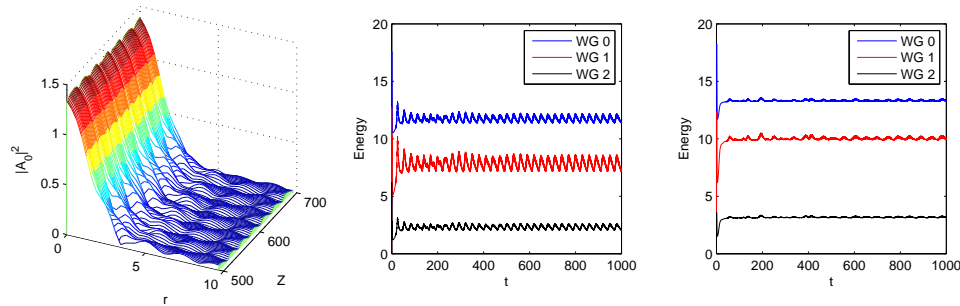


Fig. 6. A time-periodic breathing solution (left panel), along with the energy fluctuations of the radially symmetric simulations (center panel), and energy fluctuations of the full governing equation simulations (right panel). The mean value of the energy fluctuations in both radial and cartesian cases are similar in magnitude, and both settle into periodic orbits.

time, the system reaches a steady state configuration created by two pulses being spaced far enough apart so as to be effectively non-interacting. Thus, we have obtained a similar pulse-splitting behavior in the two-dimensional array to the one-dimensional array. The pulse splitting process in Fig. 7 is illustrated in the second movie (Media 2). The intensity in the all three waveguides (0th, 1st and 2nd) is included in the left, middle and right panels respectively. This process has been repeated to obtain and three- and four-pulse solutions. For large enough gains, the waveguide should be able to produce a generic N -pulse solution. Note that the splitting process generates non-radially symmetric solutions in the slab waveguide.

For all of the solutions discussed above, the qualitative structure of the light-bullets are relatively insensitive to impact of noise-like perturbation. For instance, a stable single-pulse solution will remain a stable single-pulse solution even when subjected to a large noise-like perturbations. Due to the translational symmetry inherent in this system, the pulse may translate until the perturbation has been attenuated. However, it will retain the same radial hyperbolic secant like envelope it previously had once the system returns to a steady state. Mathematically, it appears to be orbitally stable. For multi-pulse solutions, the interaction between pulses allows for more complex behaviors to exhibit themselves, and the stability of the pulses is less well established. However, if the pulses are sufficiently far apart such that the inter-pulse interaction is negligible the pulses again retain their radially symmetric (hyperbolic secant like) shape and orbital stability. Outside of this limiting case, the dynamics of multi-pulse solutions is

presently being studied.

IV. CONCLUSION

We demonstrate that mode-locking of light bullets is possible within a planar waveguide array structure. The WGAML has been heuristically extended from one propagation and time variable to one propagation and two transverse spatial variables. This extension requires the physical reinterpretation of several of the terms in the WGAML, resulting in mode-locked pulses which are fundamentally balanced with diffraction and self-phase modulation. Ultimately, the pulses obtained by this model correspond to high intensity spatially-confined solutions as opposed to the short femtosecond pulses predicted by the WGAML model. Using this model, we have found that this type of waveguide array may be used to create stable three-dimensional modelocked light bullets for a broad range of parameters. Indeed, the generated mode-locked states appear to be global attractors to the planar waveguide array system. The stability of these pulses persists for a wide range of gains, but eventually stability is lost and the system achieves a periodic breather state. For larger gains, the breather solution loses stability and multiple-pulse solutions are formed. Most importantly, as the initial condition for all these solutions is noise, this type of laser configuration is a candidate for the production of three-dimensional light bullets using passive mode-locking techniques. Additionally, the mode-locked bullets are done in a cavity-less physical geometry since no mirrors are required to form a cavity. From a technological point of view, one can also consider ramping the current injection so as to induce controlled movement of the cavity bullets. This opens

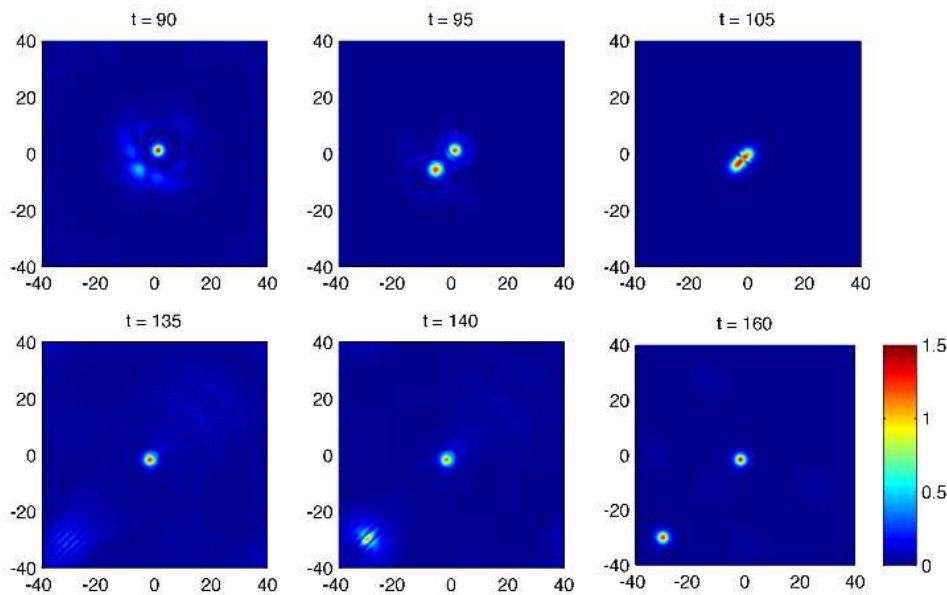


Fig. 7. Dynamics of pulse splitting for the negative-diffraction regime with $g_0 = 100$. The value of gain is too large to support either single-pulse stationary or time periodic solutions. The single pulse is unable to divide into two as shown the top row of images. Instead, an external seed, due to noise or other physical effects, is required to generate the second pulse. The two-pulse scenario is the long-time steady state solution of the system after the initial transients decay as observed.

the door for many photonic switching and optical processing operations where moving cavity solitons are of critical importance. This work also fits in the broader context of pattern forming optical systems for which cavity solitons and light bullets are of special interest. In this context, the present work demonstrates a novel technique for generating and stabilizing localized solutions. These solutions, their interactions and stability will be considered in greater depth elsewhere. Given current technologies, it is envisioned that such a geometry and experimental configuration can be achieved in practice, making the WGAML a promising photonic device for applications.

REFERENCES

- [1] D. N. Christodoulides and R. I. Joseph, "Discrete self-focusing in nonlinear arrays of coupled waveguides," *Opt. Lett.* **13**, 794-796 (1988).
- [2] D. Christodoulides, F. Lederer, and Y. Silberberg, "Discretizing light behaviour in linear and nonlinear waveguide lattices," *Nature* **424**, 817-823 (2003)
- [3] H. S. Eisenberg, Y. Silberberg, R. Morandotti, A. R. Boyd and J. S. Aitchison, "Discrete spatial optical solitons in waveguide arrays," *Phys. Rev. Lett.* **81**, 3383-3386 (1998).
- [4] A. B. Aceves, C. De Angelis, T. Peschel, R. Muschall, F. Lederer, S. Trillo, and S. Wabnitz, "Discrete self-trapping soliton interactions, and beam steering in nonlinear waveguide arrays," *Phys. Rev. E* **53**, 1172-1189 (1996).
- [5] H. S. Eisenberg, R. Morandotti, Y. Silberberg, J. M. Arnold, G. Pennelli, and J. S. Aitchison, "Optical discrete solitons in waveguide arrays. 1. Soliton formation," *J. Opt. Soc. Am. B* **19**, 2938-1944 (2002).
- [6] U. Peschel, R. Morandotti, J. M. Arnold, J. S. Aitchison, H. S. Eisenberg, Y. Silberberg, T. Pertsch, and F. Lederer, "Optical discrete solitons in waveguide arrays. 2. Dynamics properties," *J. Opt. Soc. Am. B* **19**, 2637-2644 (2002).
- [7] D. Hudson, K. Shish, T. Schibli, J. N. Kutz, D. Christodoulides, R. Morandotti and S. Cundiff) "Nonlinear femtosecond pulse reshaping in waveguide arrays," *Opt. Lett.* **33**, 1440-1442 (2008)
- [8] S. Droulias, K. Hizanidis, D. N. Christodoulides, and R. Morandotti, "Waveguide array-grating compressors," *App. Phys. Lett.* **87**, 131104 (2005).
- [9] M. O. Williams, M. Feng, J. N. Kutz, K. Silverman, R. Mirin and S. Cundiff, "Intensity Dynamics in Semiconductor Laser Arrays," *OSA Nonlinear Optics 2009 Technical Digest JTUB14* (2009)
- [10] J. N. Kutz, *Mode-Locking of Fiber Lasers via Nonlinear Mode-Coupling*, vol. 661 of *Lecture Notes in Physics* (Springer Berlin / Heidelberg, 2005).
- [11] J. Proctor and J. N. Kutz, "Theory and Simulation of Passive Mode-locking with Waveguide Arrays," *Optics Letters* **13**, 2013-2015 (2005).
- [12] J. N. Kutz and B. Sandstede, "Theory of passive harmonic mode-locking using waveguide arrays," *Opt. Express* **16**, 636-650 (2008).
- [13] B. G. Bale, J. N. Kutz and B. Sandstede, "Optimizing waveguide array mode-locking for high-power fiber lasers," *IEEE J. Sel. Top. Quantum Electron.* **15** 220-231 (2009).
- [14] See the Fundamentals, Functionalities, and Applications of Cavity Solitons (FunFACS) webpage for a complete overview of current and potential methods and realizations of generating localized optical structures: www.funfacs.org.
- [15] Y. Tanguy, T. Ackemann, W. J. Firth, and R. Jäger, "Realization of a Semiconductor-Based Cavity Soliton Laser," *Phys. Rev. Lett.* **100**, 013907 (2008).
- [16] S. Barland, J. Tredicce, M. Brambilla, L. Lugiato, S. Balle, M. Giudici, T. Maggipinto, L. Spinelli, G. Tissoni, T. Knödl, M. Müller and R. Jäger, "Cavity solitons as pixels in semiconductor microcavities," *Nature* **419**, 699-702 (2002).
- [17] V. B. Taranenko and C. O. Weiss, "Incoherent optical switching of semiconductor resonator solitons," *Appl. Phys. B* **72**, 893-895 (2001).
- [18] S. Barbay, Y. Ménesguen, X. Hachair, L. Lery, I. Sagnes and R. Kuszelewics, "Incoherent and coherent writing and erasure of cavity solitons in an optically pumped semiconductor amplifier," *Opt. Lett.* **31**, 1504-1506 (2006).
- [19] X. Hachair, L. Furfaro, J. Javaloyes, M. Giudici, S. Balle and J. Tredicce, "Cavity-solitons switching in semiconductor microcavities," *Phys. Rev. A* **72**, 013815 (2005).
- [20] U. Keller and A. C. Tropper, "Passively modelocked surface-emitting semiconductor lasers," *Phys. Reports* **429**, 67-120 (2006).
- [21] J. Marangos, "Slow Light in Cool Atoms," *Nature* **397**, 559-560 (1999).
- [22] J. T. Mok, C. M. de Sterke, I. C. M. Liter, and B. J. Eggleton, "Dispersionless slow light using gap solitons," *Nature Physics* **2**, 775-780 (2006).
- [23] P. Y. P. Chen, B. A. Malomed, and P. L. Chu, "Trapping Bragg solitons by a pair of defects," *Phys. Rev. E* **71**, 066601 (2005).
- [24] A. Yariv, *Quantum Electronics* (John Wiley and Sons, 1988).
- [25] L. Rahman and H. Winful, "Nonlinear dynamics of semiconductor laser arrays: a mean field model," *Quantum Electronics, IEEE Journal of* **30**, 1405-1416 (1994).
- [26] P. Kockaert, P. Tassin, G. van der Sande, I. Veretennicoff, and M. Tlidi, "Negative diffraction pattern dynamics in nonlinear cavities with left-handed materials," *Phys. Rev. A* **74**, 033822 (2006).